American Journal of Astronomy and Astrophysics
2025, Vol. 12, No. 1, pp. 9-20
https://doi.org/10.11648/j.ajaa.20251201.12

Research Article

Description of Lorentz Transformations, the Doppler Effect, Hubble's Law, and Related Phenomena in Curvilinear Coordinates by Generalized Biquaternions

Alimzhan Kholmuratovich Babaev[1, 2, *]

[1]Department Physics, National University of Uzbekistan, Tashkent, Republic of Uzbekistan

[2]Department of Applied Mathematics and Computer Science, Novosibirsk State Technical University, Novosibirsk, Russian Federation

Abstract

This paper presents the derivation of Lorentz transformations in curvilinear coordinates utilizing generalized biquaternions. Generalized biquaternions are rotations in curvilinear coordinates, including on the *tx*, *ty*, and *tz* planes. These space-time rotations are precisely the Lorentz transformations in curvilinear coordinates. The orbital rotation of the source and/or receiver, which mathematically represents the Lorentz transformation in spherical coordinates, is identified as the cause of the transverse Doppler effect. The change in wave frequency, specifically the "redshift," results in nonlinearities of Hubble's law manifesting as phenomena such as accelerated and anisotropic expansion of the universe, aberration, and wave polarization. Apparently, redshift exists even without radial expansion of the universe, i.e., without the "Big Bang". The reasons for the accelerated expansion of the universe, the anisotropic (angular) distribution of relic radiation, and the polarization of light from distant stars become clear in this approach. This greatly simplifies the mathematical description and understanding of the supposedly complex processes occurring in the universe.

Keywords

Biquaternion, Lorentz Transformation, Redshift, Hubble's Law, Universe Expansion, Aberration, Starlight Polarization

1. Introduction

The cause of the wave frequency shift is attributed to the satellite's orbital motion, specifically the transverse motion of the signal source in a direction perpendicular to the observer. This phenomenon is known as the transverse Doppler effect [1]. The signal frequency offset (redshift) is a function of the orbital altitude and velocity of the satellite: $\Delta\omega = f(h, v)$. Corrections [2] to adjust the data are consistently incorporated into the calculations in satellite navigation.

The classical formulation of the transverse Doppler effect (in the Cartesian coordinate system) represents a significant simplification that constrains the generalization of this principle to elucidate numerous phenomena.

The objective of this study is to derive the Lorentz transformation [3] and its associated phenomena, namely the Doppler effect and aberration, in a generalized form using curvilinear coordinates. This comprehensive approach offers

*Corresponding author: prepadamira@gmail.com (Alimzhan Kholmuratovich Babaev)

Received: 11 December 2024; **Accepted:** 27 December 2024; **Published:** 22 January 2025

universal applicability and facilitates a more profound understanding of various mechanisms, including the accelerated [4] and anisotropic [5] expansion of the Universe, as well as the nonlinear nature of the Hubble law and parameter [6].

2. Results

2.1. Biquaternions in Cartesian Coordinates

In abstract (Clifford) algebra, rotations and transformations on planes in pseudo-Euclidean space are given by formulas:

$$x' = R_\alpha x \tilde{R}_\alpha \quad (1)$$

$$\text{or } x = \tilde{R}_\alpha x' R_\alpha \quad (2)$$

Here R_α is a biquaternion, $\bar{R}_\alpha$ is the inverse or complex-conjugate biquaternion [7]:

$$R_\alpha(\tilde{R}_\alpha) = I\, cosh\frac{I\eta_\alpha+\gamma\varphi_\alpha}{2} \pm \gamma_\alpha\gamma_0\, sinh\frac{I\eta_\alpha+\gamma\varphi_\alpha}{2} \quad (3)$$

$$\text{or } R_\alpha(\bar{R}_\alpha) = exp\,(\pm\gamma_\alpha\gamma_0 z_\alpha/2) \quad (4)$$

I is a unit 4 x 4 matrix; γ_0, γ_α (α =1, 2, 3) are Dirac matrices; $\gamma = \gamma_0\gamma_1\gamma_2\gamma_3$ is a matrix analog of the imaginary unit: $\gamma^2 = -I$; $\gamma_\alpha\gamma_0 z_\alpha/2$ is a bivector;

$x = \sum_{i=0}^{3} \gamma_i \cdot x^i$ is the space-time vector in the stationary coordinate system (K); $x' = \sum_{i=0}^{3} \gamma_i \cdot x'^i$ is the same vector in the moving coordinate system (K'); $z_\alpha = I\,\eta_\alpha + \gamma\,\varphi_\alpha$ is a complex matrix.

φ_α are "purely spatial" rotations on the *x0y*, *y0z*, and *z0x* planes. Since we will only consider Lorentz transformations, we will omit these rotations in the following. η_α are angles of rotation of the *t0x*, *t0y*, and *t0z* planes, or so-called rapidities.

It is obvious that

$$R_\alpha R_\alpha^{-1} = R_\alpha \bar{R}_\alpha = I \quad (5)$$

The algorithm ((1) and/or (3)) is explained in various sources, such as [8].

Note: If there is no sum sign ($\Sigma_\alpha x_\alpha$), then there is no summation, i.e., no summation over repeated indices (Einstein's summation). For example, there is no summation over α in R_α $\bar{R}_\alpha$ or $g_{\alpha\alpha}\, k^\alpha\, x^\alpha$.

2.2. Biquaternions in Generalized Form

The generalization of the transformations (1) and (3) in curvilinear coordinates will be the following formulas:

$$x' = \mathcal{R}_\alpha x \tilde{\mathcal{R}}_\alpha \quad (6)$$

$$\text{or } x = \tilde{\mathcal{R}}_\alpha x' \mathcal{R}_\alpha \quad (7)$$

Here $\mathcal{R}_\alpha$ and $\tilde{\mathcal{R}}_\alpha$ are a biquaternion and an inverse biquaternion in a generalized form [9]:

$$\mathcal{R}_\alpha(\tilde{\mathcal{R}}_\alpha) = \frac{1}{|\tau_{\alpha 0}|}\left(I|\tau_{\alpha 0}|\, cosh\frac{z_\alpha}{2} \pm \tau_{\alpha 0}\, sinh\frac{z_\alpha}{2}\right) \quad (8)$$

$x = \sum_{i=0}^{3} e_i\, x^i$ is a 4-vector in a fixed basis K; $x' = \sum_{i=0}^{3} e_i\, x'^i$ is the same vector in the moving basis K'; $\tau_{\alpha 0} = e_\alpha \wedge e_0$ is the bivector, i.e. the outer product of vectors e_α and e_0 [10];

$|\tau_{\alpha 0}| = |e_\alpha \wedge e_0| = I(g_{\alpha 0}\, g_{\alpha 0} - g_{00}\, g_{\alpha\alpha})^{0.5}$ is the modulus ("length") of the bivector $e_\alpha \wedge e_0$ [11]; g_{ij} is a matric tensor; e_i are vectors in the system of curvilinear coordinates; $\wedge$ and $\bullet$ are symbols of outer and inner products of vectors [10].

The set of four such vectors $\{e_i\}$ forms a local basis (frame) in the 4-dimensional space. It is obvious that the biquaternions (8) satisfy the condition:

$$\mathcal{R}_\alpha \bullet \tilde{\mathcal{R}}_\alpha = I$$

Note. The name "vector" for e_i is conventional. In reality, e_i are 4 x 4 matrices related to Dirac matrices through coordinate transformation functions X_j (q^i):

$$e_i = \sum_{j=0}^{3} \frac{\partial x_j}{\partial q^i}\gamma_j$$

2.3. Lorentz Transformation in Generalized Form

Let us find the explicit form of the transformation (7). Let us substitute the biquaternions x′ and x (8) into (7).

According to Clifford's double cross product [2]

$$z\bullet(x \wedge y) = -(x \wedge y)\bullet z = (z \bullet x)\, y - (z \bullet y)x \quad (9),$$

we can write

$$x = \tilde{\mathcal{R}}_\alpha \bullet x' \bullet \mathcal{R}_\alpha = \tilde{\mathcal{R}}_\alpha \bullet \tilde{\mathcal{R}}_\alpha \bullet x' \quad (10)$$

Indeed, the identity $x' \bullet \mathcal{R}_\alpha = \tilde{\mathcal{R}}_\alpha \bullet x'$ is the place to be, since vectors $e_0 x'^0$ and $e_\alpha x'^\alpha$ commutate with $I(|\, e_\alpha \wedge e_0|\cosh(z_\alpha/2)$ but anticommutate with $I(e_\alpha \wedge e_0)\sinh(z_\alpha/2)$.

In curvilinear coordinates, the products of $e_0 \bullet \tau_{\alpha 0}$ and $e_0 \bullet \tau_{\alpha 0}$ are [12]:

$$\begin{cases} e_0 \bullet \tau_{\alpha 0} = e_0 \bullet (e_\alpha \wedge e_0) = (e_0 \bullet e_\alpha)e_0 - (e_0 \bullet e_0)e_\alpha = -g_{00}e_\alpha \\ e_\alpha \bullet \tau_{\alpha 0} = e_\alpha \bullet (e_\alpha \wedge e_0) = (e_\alpha \bullet e_\alpha)e_0 - (e_\alpha \bullet e_0)e_\alpha = g_{\alpha\alpha}e_0 \end{cases} \quad (11)$$

For simplicity, we will consider an orthogonal coordinate system, i.e., $e_i \bullet e_j = g_{ij}$, if $i=j$ and $e_i \bullet e_j = 0$, if $i \neq j$. Accordingly $|\tau_{\alpha 0}| = I(-g_{00}\, g_{\alpha\alpha})^{0.5}$.

Then from equation (10) we get

$$e_0 x^0 + e_\alpha x^\alpha = \frac{I\tau_{\alpha 0}^2 cosh\eta_\alpha + |\tau_{\alpha 0}|\tau_{\alpha 0} sinh\eta_\alpha}{\tau_{\alpha 0}^2} \bullet (e_0 x'^0 + e_\alpha x'^\alpha)$$

We substitute (11.1) and (11.2) into this equality. Multiplying the brackets and simplifying, we get

$$x\tau_{\alpha 0}^2 = e_0\tau_{\alpha 0}^2 cosh\eta_\alpha x'^0 + e_\alpha\tau_{\alpha 0}^2 cosh\eta_\alpha x'^\alpha + \\ + e_\alpha g_{00}|\tau_{\alpha 0}| sinh\eta_\alpha x'^0 - g_{\alpha\alpha} e_0 |\tau_{\alpha 0}| sinh\eta_\alpha x'^\alpha$$

Separating this equality by vectors e_0 and e_α and simplifying, we get the Lorentz transformation in curvilinear coordinates:

$$\begin{cases} x^0 = cosh\eta_\alpha \cdot x'^0 + |\tau_{\alpha 0}|/g_{\alpha\alpha} \cdot sinh\eta_\alpha \cdot x'^\alpha \\ x^\alpha = cosh\eta_\alpha \cdot x'^\alpha - |\tau_{\alpha 0}|/g_{\alpha\alpha} \cdot sinh\eta_\alpha \cdot x'^0 \end{cases} \quad (12)$$

Formula (12) is the Lorentz transformation in generalized form.

2.4. Generalized Form of the Doppler Effect and Aberration

Now we can derive the Doppler effect in curvilinear coordinates from (12). The change of frequency and direction of propagation (aberration of light) of a spherical monochromatic wave are determined by the condition of equality of phases of the same wave in both frames of reference [13]:

$$g_{00}k'^0 x'^0 + g_{\alpha\alpha}k'^\alpha x'^\alpha = g_{00}k^0 x^0 + g_{\alpha\alpha}k^\alpha x^\alpha \quad (13)$$

Substituting the values x^0, x^α from (12) into (13) and simplifying, we obtain:

$$g_{00}k'^0 x'^0 + g_{\alpha\alpha}k'^\alpha x'^\alpha =$$

$$= g_{00}k^0 cosh\eta_\alpha \cdot x'^0 - k^\alpha |\tau_{\alpha 0}| sinh\eta_\alpha \cdot x'^0 +$$

$$+ k^0 |\tau_{\alpha 0}| sinh\eta_\alpha \cdot x'^\alpha + g_{\alpha\alpha}k^\alpha cosh\eta_\alpha \cdot x'^\alpha$$

By comparing the coefficients of the same variables, we have:

$$\begin{cases} k'^0 = k^0 cosh\eta_\alpha - |\tau_{\alpha 0}|/g_{\alpha\alpha} \cdot k^\alpha sinh\eta_\alpha \\ k'^\alpha = k^\alpha cosh\eta_\alpha + |\tau_{\alpha 0}|/g_{\alpha\alpha} \cdot k^0 sinh\eta_\alpha \end{cases} \quad (14)$$

Formula (14.1) is the Doppler effect, and (14.2) is the aberration of the wave.

The plane $e_\varphi M e_\theta$ touches the surface $l l_\varphi M l_\theta$ at the point M. For small angles $d\theta$ and $d\varphi$, the arcs $l_\varphi = r \cdot sin\theta \cdot d\varphi$ and $l_\theta = r \cdot d\theta$ are a little different from straight lines. As we are considering an orthogonal coordinate system, all axes (including the time axis) are perpendicular to each other. Therefore, we take the rotation in the plane $t\ l_\theta$ as in the classical case (in pseudo-Euclidean space):

$$cosh\eta_\theta = (1 - \beta^2_\theta)^{-0.5}$$

$$sinh\eta_\theta = \beta_\theta (1 - \beta^2_\theta)^{-0.5}$$

$$tanh\eta_\theta = \beta_\theta$$

$\beta_\theta = v_\theta / c$. v_θ is the linear velocity of system v_φ relative to system K in the direction of tangent vector e_θ. c is light velocity.

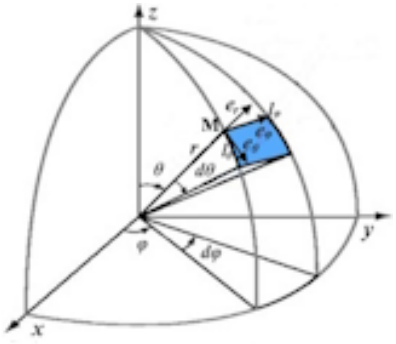

Figure 1. *Tangent plane.*

Note. We will find the geometrical and physical meaning of the functions $cosh\eta_\alpha$, $sinh\eta_\alpha$, and $tanh\eta_\alpha$ in (12) and (14) (Figure 1) in the spherical coordinate system.

$$Also\ cosh\eta_\varphi = (1 - \beta^2_\varphi)^{-0.5}$$

$$sinh\eta_\varphi = \beta_\varphi (1 - \beta^2_\varphi)^{-0.5}$$

$$tanh\eta_\varphi = \beta_\varphi$$

$\beta_\varphi = v_\varphi / c$. v_φ is the linear velocity of the system K' relative to the system K in the direction of the tangent vector e_φ.

Since r is a straight line segment, the rotation in the plane $t0r$ does not differ from the classical case:

$$cosh\eta_r = (1 - \beta^2_r)^{-0.5}$$

$$sinh\eta_r = \beta_r (1 - \beta^2_r)^{-0.5}$$

$\beta_r = v_r / c$. v_r is the velocity along r.

3. Calculations

We will not give Lorentz transformations and wave aberrations in Cartesian coordinates. The reference of rotations on the $t0x$, $t0y$, $t0z$ planes in Minkowski space where $g_{00} = 1$, $g_{11} = g_{22} = g_{33} = -1$ and $|\tau_{\alpha 0}| = I\ (-g_{00}\ g_{\alpha\alpha})^{0.5} = 1$ can be found in [13].

3.1. Lorentz Transformations and the Doppler Effect in the Time-Spherical Coordinate System: ct, r, θ, φ (Figure 2)

Let us find the form of the Lorentz transformation (12) and the Doppler effect (14.1) in the time-spherical coordinate

system: $q^0 = ct$ is time or zero axis; $q^1 = r$ is the radius vector; $q^2 = \theta$ is zenith or polar angle; $q^3 = \varphi$ is the azimuthal angle. $0 < t \le \infty$, $0 \le r \le \infty$, $0 \le \theta \le \pi$, $0 \le \varphi \le 2\pi$.

Let $\alpha = 3$, i.e., $x'^0 = ct'$, $x^0 = ct$, $x'^3 = \varphi'$, $x^3 = \varphi$, $g_{00} = 1$, $g_{33} = -r^2 sin^2\theta$, $|\tau_{30}| = r\, sin\theta$.

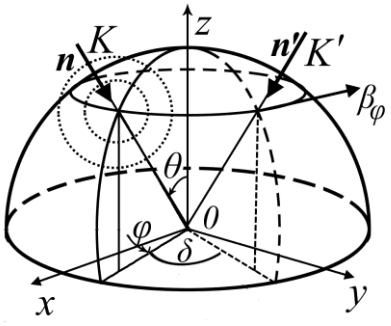

Figure 2. *Wave aberration.*

Then, from (12), we obtain the Lorentz transformations for the motion in the azimuthal plane with the velocity β_φ.

$$\begin{cases} ct = (ct' + r \cdot sin\theta \cdot \beta_\varphi \cdot \varphi')/\sqrt{1-\beta_\varphi^2} \\ \varphi = (\varphi' + \frac{\beta_\varphi}{r \cdot sin\theta} \cdot ct')/\sqrt{1-\beta_\varphi^2} \end{cases} \quad (15)$$

Let's find the type of Doppler effect and aberration. Our first objective is to determine the wave vector type for azimuthal motion β_φ ($\beta_r = \beta_\theta = 0$) (Figure 3). $\beta\varphi$ is a velocity of system K' relative to K that is tangent to the arc (along φ).

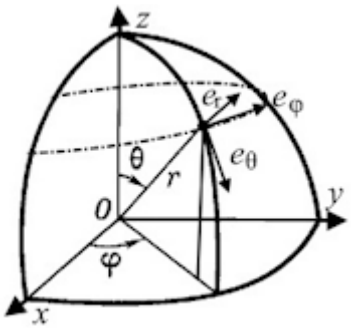

Figure 3. *Body movement along axes.*

The wave vector n is perpendicular to the front of a spherical monochromatic wave. The angle between n and x is equal to φ. The angle between vector n' and x is equal to $\varphi + \delta$.

The aberration angle δ is the angle between the vectors n and n'.

From equation (14) we get

$$\begin{cases} \omega' = \omega \cdot (1 - r \cdot sin\theta \cdot \beta_\varphi)/\sqrt{1-\beta_\varphi^2} \\ \omega' \cdot cos\delta = \omega \cdot (1 - \frac{\beta_\varphi}{r \cdot sin\theta})/\sqrt{1-\beta_\varphi^2} \end{cases} \quad (16)$$

The aberration angle δ is the difference between the angle of wave incidence from the source and the observed angle, which varies due to the rotation of the receiver (e.g., the Earth) in orbit.

(16.1) is the Lorentz transformation, and (16.2) is the aberration of the wave at the azimuthal velocity of the source (receiver). The aberration angle δ is defined relative to the wave vector n in formula (16.2).

We find δ relative to the observer (point 0) (Figure 3). Since $\angle z\hat{}n = \varphi$ and $\angle z\hat{}n' = \varphi + \delta$, then

$$k^3 = \frac{\omega}{c} cos\varphi,\ k'^3 = \frac{\omega'}{c} \cos(\varphi + \delta),\ k^0 = \frac{\omega}{c},\ k'^0 = \frac{\omega'}{c}.$$

Then equations (14) for $\alpha = 3$ can be written as:

$$\omega' = \omega \cdot (cosh\eta_\varphi - r \cdot sin\theta \cdot cos\varphi \cdot sinh\eta_\varphi)$$

$$\omega' \cos(\varphi + \delta) = \omega(cos\varphi \cdot cosh\eta_\varphi - \frac{1}{r \cdot sin\theta} \cdot sinh\eta_\varphi)$$

Substituting the first equation into the second one, we get:

$$\cos(\varphi + \delta) = \frac{cos\varphi - \frac{\beta_\varphi}{r \cdot sin\theta}}{1 - r \cdot sin\theta \cdot cos\varphi \cdot \beta_\varphi} \quad (17)$$

On the radial motion of the wave source or receiver ($g_{00} = 1$, $g_{11} = -1$), we obtain the relativistic Einstein aberration formula [14] from (17).

If $\varphi = \pi/2$, then from (17) we get

$$sin\delta = \beta_\varphi / r \cdot sin\theta \quad (18)$$

Let's calculate the annual aberration of the stars. We take $r = \rho/1$au and $\theta = \pi/2$ in formula (18).

1 au = 149 597 870 700 m is an astronomical unit.

On aphelion, the Earth's orbital velocity is $\beta\varphi = 29.29/3 \cdot 10^5$, and it's $\rho = 1.016$ au from the Sun [15]. On perihelion, the Earth's orbital velocity is $\beta\varphi = 30.29/3 \cdot 10^5$ and the distance to the Sun is $\rho = 0.98329$ *au* [15].

Calculations using the formula (18) show that the annual aberration angle is equal to:

$\delta_a = 19.80753477''$-for afelius; $\delta_p = 21.17978416''$-for perihelion; $\bar{\delta} = 20.49365946''$– mean value;

$\delta_{exp} = 20.49552''$ is the officially accepted annual aberration value [16].

The measurement error ($\Delta = (\delta_{exp} - \bar{\delta})/\delta_{exp}$) in the calculation of δ is less than $\Delta < 10^{-3}\%$.

We will not consider the case $\alpha = 2$, i.e., motion along the direction of the vector e_θ ($x'^0 = ct'$, $x'^2 = \theta'$, $x^0 = ct$, $x^2 = \theta$, $g_{00} = 1$, $g_{22} = -r^2$, $|\tau_{20}| = r$), since $\alpha = 2$ is a special case of $\alpha = 3$.

Also the case $\alpha = 1$ (radial motion of the source and/or receiver) does not differ from the classical case (Cartesian coordinate system).

3.2. Hubble's Law

We now find the dependence of the redshift

$z = (\omega-\omega')/\omega'$ on the distance r between the source and receiver of the wave.

Substituting (16.1) into z, we get

$$z = \frac{sin\theta \cdot \beta_\varphi}{1-r \cdot sin\theta \cdot \beta_\varphi} \cdot r \quad (19)$$

To be precise, the galaxy's recessional velocity v is by no means equal to, but only proportional to $c \cdot z$ (the product of the speed of light c and the redshift z). Therefore, we multiply formula (19) by $k \cdot c$ and obtain the dependence of the galaxy scattering velocity v on the distance between them r, i.e., Hubble's law [17]:

$$v = k \cdot c \cdot \frac{sin\theta \cdot \beta_\varphi \cdot r}{1-r \cdot sin\theta \cdot \beta_\varphi} \quad (20)$$

For "small distances" (up to 4 *Mpc*), the coefficient k = 291.2583845 is determined by the least square method from the experiment [20], which is given in Table 1 (light yellow columns).

Table 1. *Experimental data for Hubble's law.*

Experimental data for Hubble's law					
from [20]		**from [21]**		**from [20]+[21]**	
r	**v**	**r**	**v**	**r**	**v**
0	-25	015.0	1380	000	-25
0.032	170	031.3	2304	000.032	170
0.034	290	038.7	3294	000.034	290
0.214	-130	039.5	3149	000.214	-130
0.263	-70	043.2	3272	000.263	-70
0.275	-202.5	045.1	3106	000.275	-202.5
0.45	200	050.9	4398	000.45	200
0.5	280	053.3	3545	000.5	280
0.62	300	056.0	4124	000.62	300
0.63	200	057.3	4869	000.63	200
0.67	400	058.0	4227	000.67	400
0.79	290	058.3	4061	000.79	290
0.8	300	062.2	4749	000.8	300
0.9	215.1665	066.6	4924	000.9	215.1665
1.	760.	066.7	4730	001	760
1.1	537.5	066.8	4847	001.1	537.5
1.16	800	068.2	4820	001.16	800
1.2	580	071.8	5424	001.2	580
1.24	600	074.3	4982	001.24	600
1.27	730	077.9	5434	001.27	730
1.4	500	082.4	6673	001.4	500
1.42	700	085.6	7143	001.42	700
1.49	810	088.4	7016	001.49	810
1.52	650	088.6	5935	001.52	650
1.53	800	089.2	6709	001.53	800

Experimental data for Hubble's law

from [20]		**from [21]**		**from [20]+[21]**	
r	**v**	**r**	**v**	**r**	**v**
1.7	960	096.7	7241	001.7	960
1.73	650	102.1	7765	001.73	650
1.74	940	114.9	8930	001.74	940
1.79	800	117.1	9801	001.79	800
2	810	119.7	8604	002	810
2.06	900	121.5	7880	002.06	900
2.23	1140	127.8	8691	002.23	1140
2.35	1100	132.7	10446	002.35	1100
2.37	1300	134.7	9065	002.37	1300
3.45	1800	136.0	9024	003.45	1800
		149.9	10715	015.0	1380
		151.4	10696	031.3	2304
		158.9	12012	038.7	3294
		176.8	12871	039.5	3149
		183.9	13707	043.2	3272
		185.6	14634	045.1	3106
		19.80	1088	050.9	4398
		198.6	15055	053.3	3545
		20.70	1607	056.0	4124
		202.3	14764	057.3	4869
		202.5	13518	058.0	4227
		215.4	15002	058.3	4061
		235.9	17371	062.2	4749
		236.1	15567	066.6	4924
		238.9	16687	066.7	4730
		262.2	18212	066.8	4847
		274.6	22426	068.2	4820
		280.1	18997	071.8	5424
		303.4	21190	074.3	4982
		309.5	23646	077.9	5434
		391.5	26318	082.4	6673
		467.0	30253	085.6	7143
				088.4	7016
				088.6	5935
				089.2	6709
				096.7	7241

Experimental data for Hubble's law					
from [20]		from [21]		from [20]+[21]	
r	v	r	v	r	v
				102.1	7765
				114.9	8930
				117.1	9801
				119.7	8604
				121.5	7880
				127.8	8691
				132.7	10446
				134.7	9065
				136.0	9024
				149.9	10715
				151.4	10696
				158.9	12012
				176.8	12871
				183.9	13707
				185.6	14634
				19.80	1088
				198.6	15055
				20.70	1607
				202.3	14764
				202.5	13518
				215.4	15002
				235.9	17371
				236.1	15567
				238.9	16687
				262.2	18212
				274.6	22426
				280.1	18997
				303.4	21190
				309.5	23646
				391.5	26318
				467.0	30253

In (20), all variables (z, $\beta_\varphi = v_\varphi/c$, r) are dimensionless, so we accept $r = d/R_0$. $R_0 = 14300$ *Mpc* [18] is the radius of the effective particle horizon, up to which we can see particles created since the Big Bang;

d is the distance from the object to the observer, measured in *Mpc*;

$\beta_\varphi = 24000/300000 = 0.08$ is the linear velocity at the periapsis of S4714's proper orbit [19]. This is the highest

velocity in our galaxy (Milky Way).

Then (20) has the form ($sin\theta \approx 1$):

$$v = 0.08k \cdot cd / (R_0 - 0.08d) \quad (21)$$

Figure 4 shows the approximation of the data from [20] by function (21). ■-data from [20], red dashed line-function (21). We can see that formula (21) agrees well with experiments up to distances $d \sim 4$ *Mpc*.

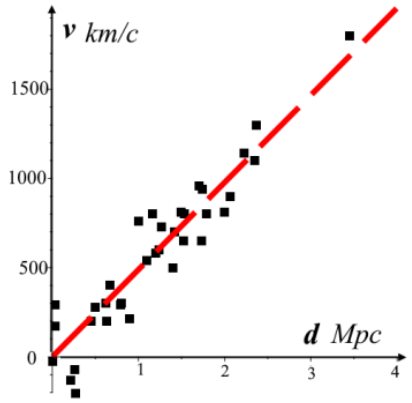

Figure 4. *Hubble's law.*

If we consider Hubble's law as before, i.e., the dependence $v \sim f(d)$ is linear (Figure 5)

$v = H(r, \theta, v_\varphi) \cdot d$,

then we get the Hubble parameter $H(r, \theta, v_\varphi)$:

$$H(d, \theta, v_\varphi) = \frac{sin\theta \cdot \beta_\varphi \cdot k \cdot c}{1 - sin\theta \cdot \beta_\varphi \cdot d} \quad (22)$$

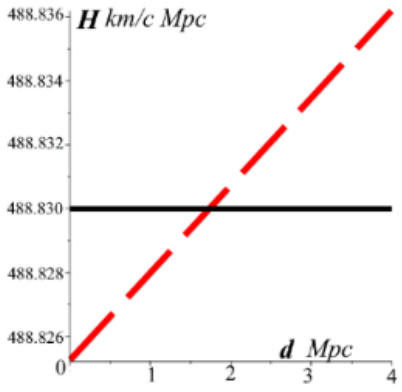

Figure 5. *Hubble parameter.*

here $\bar{H} = 488.83$ *km/c/Mpc*. ($488.825 < H(r, \theta, v_\varphi) < 488.835$) is mean value (dark line in Figure 5). This value (488.83 km/c/Mpc), calculated by formula (22), is very close to the proportionality coefficient found by Hubble (500 km/c/Mpc).

In fact, $H(r, \theta, v_\varphi)$ depends on d, θ, and v_φ. Therefore, the Hubble parameter grows weakly with increasing source-receiver distance (Figure 5).

It would be more correct to take the dependence $z \sim f(d)$ instead of $v \sim f(d)$. Hubble's law was originally derived empirically, also from the assumption that the redshift of the spectrum is due to the radial velocity of objects. In addition, the assumption was that the dependence would be linear. But formula (21) shows that Hubble's law is nonlinear: as the distance between objects increases, the "galaxy expanding velocity," or more precisely, the redshift (Hubble parameter, too), increases even at low velocities and without radial velocity, i.e., without galaxy expansion ($v_r = 0$).

At large distances (up to 500 *Mpc*), the redshift and the Hubble parameter increase further (Figure 6), red dotted line).

The small inside figure is a Hubble diagram. The red square at the origin shows the comparative scale and location of the Hubble diagram.

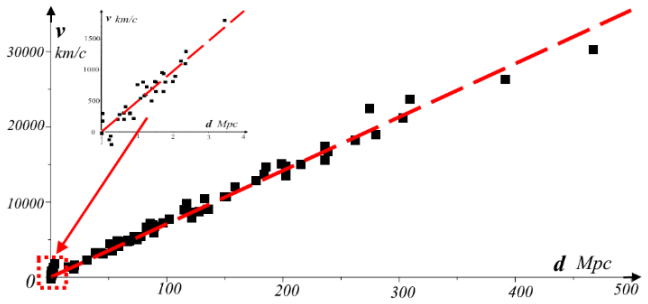

Figure 6. *Hubble's Law at Long Distances.*

The function (21) tends to infinity, i.e., it will have a singularity at $0.08\ d \rightarrow R_0$.

For distances (up to 500 *Mpc*), the coefficient k =42.21890063 is determined by the least square method from the experiment [20, 21], which is given in Table 1 (light blue columns).

The cause of redshift is not only radial motion but also an orbital motion of the source and/or receiver. Simply put, the radial recede of galaxies is not the main reason for redshift. The source and/or receiver's orbital motion is likely the primary cause of the redshift.

Now consider the dependence of redshift z on the zenith angle θ and the distance between objects d: $z \sim f(d, \theta)$.

From (20) we get

$$z = \frac{k \cdot sin\theta \cdot 0.08}{R_0 - sin\theta \cdot 0.08 \cdot d} \cdot d \quad (23)$$

Figure 7 shows the dependence: $z \sim f(d, \theta)$. The two-dimensional plot (Figure 7A) shows that z reaches a maximum at $\theta = \pi/2$ for all values of d ($d_1 > d_2 > d_3 > d_4$). Astronomers often take the angle θ (zero) not from the North Pole [22], but from the ecliptic plane, i.e., from the plane of

the Earth's orbit around the Sun. Then we should use cosθ instead of sinθ in formula (23). We'll continue that tradition.

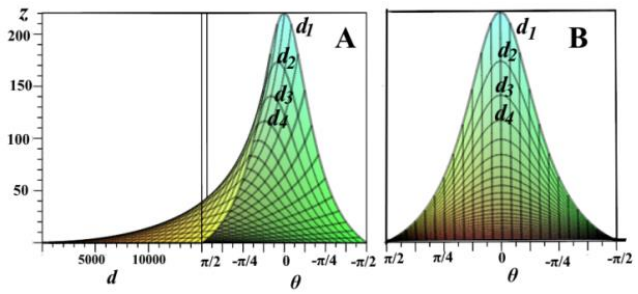

Figure 7. *Dependence z ~ f(d, θ) and its section by d.*

Figure 7B shows the projection of f (d, θ) onto the z, θ plane. The graph shows that the closer the angle θ is to the ecliptic (θ→ 0) and the larger the distance d, the larger the redshift z.

We can only observe longitude $0 \leq \varphi \leq 2\pi$ and latitude $-\pi/2 \leq \theta \leq 2\pi$ in the sky. We don't see the depth of the sky, i.e., the distance d to the celestial object. We determine it by indirect evidence (brightness, etc.). We calculate the redshift z by formula (23). However, formula (23) depends not on angle φ but on angle θ (Figure 7B).

If the dependence $z \sim f(d, \theta)$ (24) is plotted on a map of the Universe (latitude and longitude), we get the picture as in Figure 8A.

Figure 8B shows a map of the anisotropy of the relic radiation [23] in the *K*, *Ka*, *Q*, *V*, and *W* bands. A plot of z versus zenith angle θ (- 900 ≤ θ ≤900 vertically) on the latitude-longitude map is shown on the left (Figure 8A).

We see that the z maxima are centered on a narrow band for all d (red shaded band in Figure 8A). In the experiment, the "hot" (red) regions are also located in the center of the ecliptic (Figure 8B).

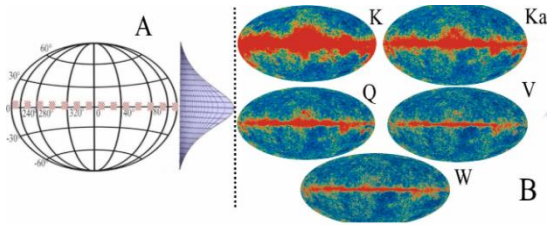

Figure 8. *Universe map in latitudes and longitudes.*

We see that the z maxima are centered on a narrow band for all *d* (red shaded band in Figure 8A). In the experiment, the "hot" (red) regions are also located in the center of the ecliptic *(*Figure 8*B)* (Figure 8B). Simply put, the observer (telescope) fixes large ("hot") z 's closer to the ecliptic and small ("cold") *z* 's farther from the ecliptic. This is similar to how an astronaut from space cannot tell the height of mountain ranges on Earth but only sees stripes where the ridges are.

Note again that the width and length of the red shaded band (Figure 8A) depend on z: narrow and short bands correspond to large z, and wide and long bands correspond to small *z*. This is visually consistent with the data on the right: *K* <*Ka* <*Q* <*V* <*W*.

The irregularity of the bands in Figure 8B (randomness, scattering) is most likely due to the random distribution of the object velocity and the proximity of the clusters. The "disorderly" arrangement of bright points in cold regions (further from the ecliptic) is probably due to a random distribution of distances d between the source and the receiver (observer).

3.3. Polarization of the Waves

The wave vector changes direction relative to the observer due to the satellite's orbital rotation. The direction of the wave vector changes by an angle δ (aberration angle) due to the rotation of the stars in their orbits and/or the rotation of the Earth around the Sun. The rotation of the source and/or receiver along the orbit is the cause of the change in the direction of the wave vector, causing the change from *n* to *n*′. This change in the direction of the wave is the cause of the transverse Doppler effect, the aberration, and the polarization of the "refracted" wave.

By analogy with geometrical optics in formula (17), we denote:

$\pi/2-\varphi = \alpha$ is the angle of incidence of the wave; $\pi/2-(\varphi+\delta) = \gamma$ is the angle of refraction of the wave;

Considering

$cos\,(\varphi + \delta) = cos\,(\pi/2 - \gamma) = sin\gamma$ and

$cos\varphi = cos\,(\pi/2 - \alpha) = sin\alpha$

and simplifying from equation (17), we get

$$\frac{sin\alpha}{sin\gamma} = \frac{1-r\cdot sin\theta\cdot sin\alpha\cdot\beta_\varphi}{1-\beta_\varphi/r\cdot sin\theta\cdot sin\alpha}$$

Let $\theta = \pi/2$. Then

$$\frac{sin\alpha}{sin\gamma} = \frac{1-r\cdot sin\alpha\cdot\beta_\varphi}{1-\frac{\beta_\varphi}{r\cdot sin\alpha}} \quad (24)$$

By analogy with Snell's law [24], let us introduce the "refractive index" of the vacuum:

$$n = \frac{1-r\cdot sin\alpha\cdot\beta_\varphi}{1-\frac{\beta_\varphi}{r\cdot sin\alpha}} \quad (25)$$

If $g_{33} = r\cdot sin\alpha = -1$ (rectangular coordinates), then (25) gives n=1– the classical "refractive index" of vacuum. In curvilinear coordinates, the refractive index of vacuum n differs from unity. For example, for an observer on Earth at aphelion n=0.9999967655 < 1, at perihelion n = 1.000003403 > 1.

Let the "incident" monochromatic wave *n* be directed along the unit vector *k* and the velocity of the wave source be along

the unit vector j. The direction of the "refracted" wave n' will be k', and the direction of the velocity n' will be j' (Figure 9).

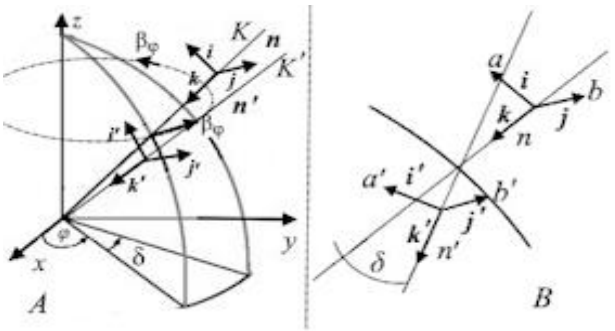

Figure 9. *Wave polarization.*

Figure 9A shows the incident wave K and the wave K' (with velocity β_φ on orbit) in a spherical coordinate system. Figure 9B shows the waves K and K' on the incision plane through a vertical plane (the azimuthal angle is φ). Note that j and j' coincide.

We directed n along k freely, at our discretion, and the velocity β_φ along j. But the choice of k', j', and i' is not free, but rigidly connected with k, j, and i.

Let's consider the electrical components of the "incident" wave:

$$E = E_0 e^{i(\hbar r - \omega t)} = E_0 \cos(\hbar r - \omega t) + iE_0 \sin(\hbar r - \omega t)$$

$\hbar$ is the wave vector.

Of course, all of the above also applies to the magnetic field.

Let's introduce vectors:

$a = E_0 \cos(\hbar r - \omega t) = ia$;

$b = Re\{iE_0 \sin(\hbar r - \omega t)\} = jb$;

$a' = E_0' \cos(\hbar r - \omega t) = ia'$;

$b' = Re\{iE_0' \sin(\hbar r - \omega t)\} = jb'$.

Then E = i ·a +j ·b, E' = i'·a' +j'·b'

Figure 9B clearly shows that the angle between a and a′ is equal to δ, as is the angle between i^i′ and between k^k′. The angle between b and b′ is zero, as is the angle between j^j′.

The projections of a′ onto a and b′ onto b are:

a'' = a· cosδ and b''=b

The polarization vector is along k. Since we have described n in the right-handed coordinate system (right-handed vector triad), n' will also be right-handed polarized.

Let's find the polarization vector P (a=b):

$$P = \frac{E_j^2 - E_i^2}{E_j^2 + E_i^2} = \frac{b^2 - a^2 cos^2\delta}{b^2 + a^2 cos^2\delta}$$

Incident wave (n) is natural, not polarized. For natural light, where waves of different polarizations are equally mixed and all directions are equal. Assuming that the polarized wave n' (after "refraction") is half the natural wave, we get:

$$P = \frac{1}{2} \cdot \frac{1 - cos^2\delta}{1 + cos^2\delta} \quad (26)$$

From formula (26), we can find the degree of polarization for annual aberration. Substituting (18) into (26) and simplifying, we get:

$$P = \frac{1}{2} \cdot \frac{sin^2\delta}{2 - sin^2\delta} = \frac{0.5}{2 \cdot sin^{-2}\delta - 1} \text{ or}$$

$$P = \frac{0.5}{2 \cdot \beta_\varphi^{-2} \cdot r^2 \cdot cos^2\theta - 1} \quad (27)$$

At aphelion (β_φ=29.29/300000, r=1.0167 *au*, θ = 0)-P_α = $2.31 \cdot 10^{-9}$. At perihelion (β_φ=30.29/300000, r=0.98329 *au*, θ = 0)-P_p = $2.64 \cdot 10^{-9}$.

We took the zenith angle from the ecliptic, following the astronomers: $sin\theta \rightarrow cos\theta$. Of course, the effects are very weak: P_α and P_p.

In general, the degree of polarization (27) depends on the distance between the source and receiver and the zenith angle (elevation angle).

The starlight polarization dependence denoted as

$$P = \left| \frac{k \cdot 0.5}{2 \cdot \beta_\varphi^{-2} \cdot (d/R_0)^2 \cdot cos^2\theta - 1} \right|, \quad (28)$$

is illustrated in Figure 10.

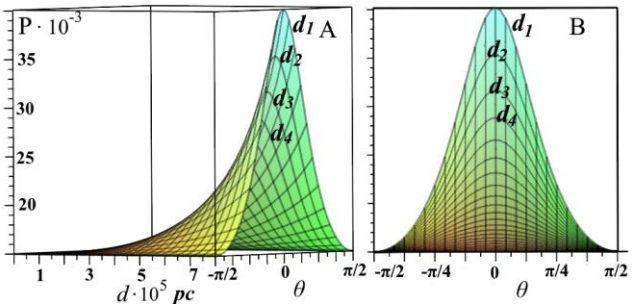

Figure 10. *Starlight polarization dependence P = f (d, θ).*

$\beta\varphi = 10^{-4}$ is Earth's average orbital velocity; R_0 =14300·106 *pc* [18]; d is distance from observer (on Earth) to wave source. k=0.03.

The degree of polarization, P, of the starlight at the moment of emission (at the beginning) is unknown. According to observations reported in [25], the degree of polarization is approximately 1.5% for stars at a distance of 1000 parsecs. Therefore, the coefficient of proportionality is taken to be k = 0.03.

It is important to note that the graphs depicted in Figure 10 of the study on starlight polarization should not be regarded as a quantitative analysis in the strict sense of the term. Rather, they serve as a visual representation of the trends in the laws of starlight polarization.

The dependences of $P \sim f(\theta)$ at $d_1 > d_2 > d_3 > d_4$ are shown in Figure 10B.

Figure 10B is an incision of the 3-dimensional Figure 10A by the plane θ: $P \sim f(d, \theta)$. It is obvious that for large d and $\theta \sim 0$, the degree of polarization P is maximum.

Figure 11 shows plots of experimental data on measurements of the degree of polarization of stars [25].

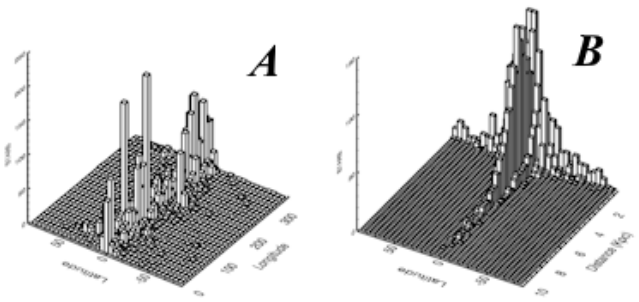

Figure 11. *Experimental data of the polarized starlight.*

Graph 10A does not conflict with Graph 11B, which is the experiment. Graph 11A doesn't contradict Graph 10B if the latter is placed on the θ, φ plane.

It is obvious that here, as in the case of the redshift (Figure 8), we also see a stripe close to the ecliptic (θ~0) (Figure 10).

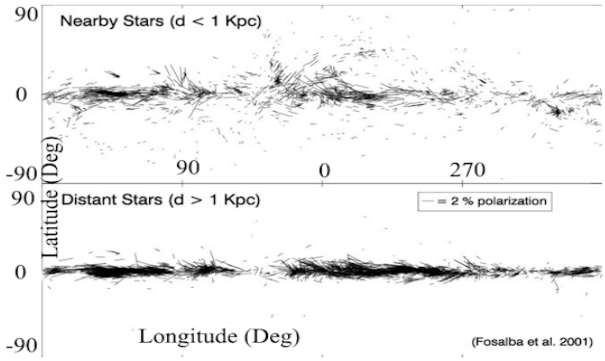

Figure 12. *CMB polarization.*

Figure 12 shows starlight polarization vectors in galactic coordinates for 5513 stars. {52} for a local cloud (upper) and for an average polarization vector over many clouds (lower).

Our calculations for measuring the degree of polarization do not include statistical hypothesis testing (due to the small sample). Nevertheless, both graphs (Figures 11 and 12) visually demonstrate the correctness of our assumption about the dependence of the degree of polarization on distance and polar angle: the greater the distance between the source and receiver of the wave and the closer the elevation angle to the ecliptic ($\theta \sim 0$), the greater the degree of polarization. In other words, large redshifts z and maximum degrees of polarization P are concentrated near the ecliptic plane.

Abbreviations

CMB	Cosmic Microwave Background
pc	Parsec
Mpc	Mega Parsec

Acknowledgments

It should be noted that I would hardly be able to compare with reality and check the plausibility of the theoretical assumptions presented in the article without the scientific works (without experimental data) of scientists such as Hubble E., Freedman W. L. and co-authors, Rosalia P., Lazarian Alex and co-authors, and also Bennett et al.

I would like to express my gratitude to my ally, my wife Lyuba Gomazkova, for correcting and formatting the Russian version of the text and formulas, for creating a cozy and comfortable working environment, and, above all, for her angelic patience.

I would like to express special thanks to SciencePG for their unpaid help and work in publishing this (not only this) article. They have become the "godfathers" of my articles for the English-speaking public.

Author Contributions

Alimzhan Kholmuratovich Babaev is the sole author. The author read and approved the final manuscript.

Conflicts of Interest

The author declares no conflicts of interest.

References

[1] Daniel Nieto Yll. Doppler shift compensation strategies for LEO satellite communication systems. Polytechnic University of Catalonia. Published 1 June 2018. https://upcommons.upc.edu/bitstream/handle/2117/123510/DanielNietoYll_Doppler_compensation_for_LEO.pdf

[2] The global positioning system, relativity, and extraterrestrial navigation Neil Ashby and Robert A. Nelson 2008. https://doi.org/10.1017/S174392130999010X

[3] Wikipedia. Lorentz transformations. https://en.wikipedia.org/wiki/Lorentz_transformation

[4] Pain, Reynald; Astier, Pierre (2012). "Observational evidence of the accelerated expansion of the Universe". *Comptes Rendus Physique*. 13 (7): 521–538. pp. 13-16 https://doi.org/10.1016/j.crhy.2012.04.009 (In French).

[5] Jacques Colin, Roya Mohayaee, Mohamed Rameez and Subir Sarkar (Nov 2019). "Evidence for anisotropy of cosmic acceleration⋆". Astronomy & Astrophysics. 631: L13. https://doi.org/10.1051/0004-6361/201936373 20.11. 2019.

[6] Freedman, W. L.; Madore, B. F. (2010). The Hubble Constant. Annual Review of Astronomy and Astrophysics. 48: 673–710. https://doi.org/10.48550/arXiv.1004.1856

[7] Sangwine, Stephen J.; Ell, Todd A.; Le Bihan, Nicolas (2010), "Fundamental representations and algebraic properties of biquaternions or complexified quaternions", Advances in Applied Clifford Algebras, 21 (3): 1–30, https://doi.org/10.48550/arXiv.1001.0240

[8] The rules of 4-dimensional perspective: How to implement Lorentz transformations in relativistic visualization. Andrew J. S. Hamilton. [gr-qc] 16 Nov 2021. https://doi.org/10.1007/s00006-022-01257-5

[9] Babaev A. Kh., Biquaternions, rotations, and spinors in the generalized Clifford algebra (in Russian). Sci-article.ru. № 45 (May) 2017. pp. 296 - 304, https://doi.org/10.24108/preprints-3112462

[10] Chris J. L. Doran. Geometric Algebra and its Application to Mathematical Physics. Sidney Sussex College. A dissertation submitted for the degree of Doctor of Philosophy in the University of Cambridge. February 1994, pages 4-6.

[11] Gaston Casanova. L'Algebre Vectorielle. Press Universitaires de France. p. 10, 19. https://books.google.ru/books?id=Es__EAAAQBAJ&pg=PA2&hl=ru&source=gbs_toc_r&cad=2#v=onepage&q&f=false

[12] Babaev A. Kh. Alternative formalism based on Clifford algebra (in Russian), SCI-ARTICLE.RU. №40 (December) 2016, pp. 34-42, https://doi.org/10.24108/preprints-3112477

[13] Landau L. D., Lifshitz E. M., The Classical Theory of Fields, Course of Theoretical Physics, vol. 2, pp. 123-127.

[14] Albert Einstein (1905) "Zur Elektrodynamik bewegter Körper", *Annalen der Physik* 17: 891; English translation. https://doi.org/10.1002/andp.19053221004

[15] Wikipedia. https://en.wikipedia.org/wiki/Earth%27s_orbit

[16] Wikipedia. https://en.wikipedia.org/wiki/Astronomical_constant

[17] Dan Scolnic, Lucas M. Macri, Wenlong Yuan, Stefano Casertano, Adam G. Riess. Large Magellanic Cloud Cepheid Standards Provide a 1% Foundation for the Determination of the Hubble Constant and Stronger Evidence for Physics Beyond Lambda CDM -2019-03-18. https://doi.org/10.48550/arXiv.1903.07603

[18] Gott III, J. Richard; Mario Jurić; David Schlegel; Fiona Hoyle; et al. (2005). "A Map of the Universe" (PDF). *The Astrophysical Journal*. 624 (2): 463–484. https://doi.org/10.1086/428890

[19] Florian Peißker, Andreas Eckart, Michal Zajaček, Basel Ali, Marzieh Parsa. S62 and S4711: Indications of a population of faint fast moving stars inside the S2 orbit -- S4711 on a 7.6 year orbit around Sgr~A* // The Astrophysical Journal. — 2020-08-11. https://doi.org/10.48550/arXiv.2008.04764

[20] Hubble E. (1929). "A relation between distance and radial velocity among extra-galactic nebulae". Proceedings of the National Academy of Sciences 15 (3): 168–173. https://doi.org/10.1073/pnas.15.3.168

[21] W. L. Freedman, B. F. Madore, B. K. Gibson, L. Ferrarese, D. D. Kelson, S. Sakai, J. R. Mould, R. C. Kennicutt Jr., H. C. Ford, J. A. Graham and others, Hubble, E. (1929). "A relation between distance and radial velocity among extra-galactic nebulae". Proceedings of the National Academy of Sciences. 15 (3): 168–173. Final Results from the Hubble Space Telescope Key Project to Measure the Hubble Constant, https://doi.org/10.48550/arXiv.astro-ph/0012376

[22] Wikipedia. https://en.wikipedia.org/wiki/Ecliptic

[23] First Year Wilkinson Microwave Anisotropy Probe (WMAP) Observations: Preliminary Maps and Basic Results, C.L. Bennett, et al., 2003ApJS..148....1B, reprint / preprint (4.4 Mb) / individual figures / ADS / astro-ph, https://lambda.gsfc.nasa.gov/product/wmap/pub_papers/firstyear/basic/wmap_cb1_images.html

[24] Wikipedia. https://en.wikipedia.org/wiki/Snell%27s_law

[25] Fosalba, Pablo; Lazarian, Alex; Prunet, Simon; Tauber, Jan A. (2002). "Statistical Properties of Galactic Starlight Polarization". *Astrophysical Journal*. 564 (2): 762–772. https://doi.org/10.1086/324297

Biography

Alimzhan Kholmuratovich Babaev defended his thesis for a PhD in physical and math sciences on the topic "Multiple collisions of particles and fragmentations of 22Ne nuclei in a photoemulsion at P/A=4.1 GeV/c" in 1989 at the Institute of Nuclear Physics of the Academy of Sciences of Uzbekistan (Tashkent). He worked at the Department of Nuclear Physics and Cosmic Rays at the National University (Tashkent, Uzbekistan) as an associate professor. Since 2000, he has worked as a lecturer at the Novosibirsk State Technical University (Novosibirsk, Russian Federation) in the Department of Higher Mathematics. At present, he is working as an independent researcher in the field of applications of methods of abstract algebra to classical and quantum field physics. He is the author (co-author) of more than 30 scientific papers published in peer-reviewed journals.

Research Field

Alimzhan Kholmuratovich Babaev: Research field: Clifford algebra, Gravity, Electromagnetism, Biquaternions and Spinor fields, Partial differential equations, Unified field theory.